Bulletin of the Seismological Society of America, Vol. 74, No. 1, pp. 79–90, February 1984

THEORETICAL STUDY OF THE EXCITATION, SPECTRAL CHARACTERISTICS, AND GEOMETRICAL ATTENUATION OF REGIONAL SEISMIC PHASES

BY MICHEL CAMPILLO, MICHEL BOUCHON, AND BERNARD MASSINON

ABSTRACT

We present a theoretical study of the generation and geometrical attenuation of regional crustal phases. We do this through the computation of seismograms in the epicentral distance range from 60 to 500 km. The geometrical attenuation of *Lg* waves with epicentral distance is of the form $r^{-0.83}$. *Pg* wave amplitudes display a much stronger decay of the form $r^{-1.5}$. The spectral density of the crustal transfer function for *Pg* waves is relatively flat for frequencies between 0.1 and 5 Hz while *Lg* wave spectra strongly fall off beyond 2 to 3 Hz.

The excitation of *Pg* wave is insensitive to the depth of the source within the crust while the *Lg* amplitude is about 50 per cent higher for a source in the upper and middle crust than in the lower crust. The amplitudes of these two phases drastically decrease when the source is below the Moho. These results illustrate the important role of wave guide played by the crust for the propagation of *Lg* and *Pg*.

We find that the geometrical attenuation of *Pg* and *Lg* waves is independent of source mechanisms. In the case of an explosion, the excitation of *Pg* is insensitive to the source depth. The *Lg* wave amplitude is small in comparison to *Pg* and Rayleigh waves and depends on the closeness of the source to an interface or to the free surface.

INTRODUCTION

In the past decade, much effort has been devoted to the study of regional seismic phases. In particular, the attenuation characteristics of *Lg* and *Pg* waves have been obtained for many regions of the world (e.g., Nuttli, 1973, 1980; Bollinger, 1979; Pomeroy and Chen, 1980; Nicolas *et al.*, 1982) and the relative excitation of these phases by earthquakes and explosions has been investigated (e.g., Pomeroy and Nowak, 1979; Gupta *et al.*, 1980; Nuttli, 1981). Most of the knowledge accumulated about these phases, however, comes from experimental work. Although theoretical investigations of *Lg* and *Pg* waves have been intensified in the past few years (Müller and Mueller, 1979; Bache *et al.*, 1981; Cara and Minster, 1981; Herrmann and Goertz, 1981; Bouchon, 1982; Langston, 1982; Olsen and Braile, 1983), their outcome still lags behind the experimental results.

The aim of this paper is to broaden our theoretical understanding of the factors governing the excitation and the propagation of these waves. This will be attempted through the calculation of synthetic seismograms. We shall rely for the computation on the discrete wavenumber representation method (Bouchon and Aki, 1977; Bouchon, 1981).

GEOMETRICAL ATTENUATION AND SPECTRAL CHARACTERISTICS OF *PG* AND *LG*

First described by Press and Ewing (1952), the *Lg* wave has been interpreted as higher mode surface wave propagation (Oliver and Ewing, 1957, 1958; Kovach and Anderson, 1964; Knopoff *et al.*, 1973; Panza and Calcagnile, 1975). Recent studies done by Bouchon (1982) and Olsen and Braile (1983) have shown that the *Lg* phase

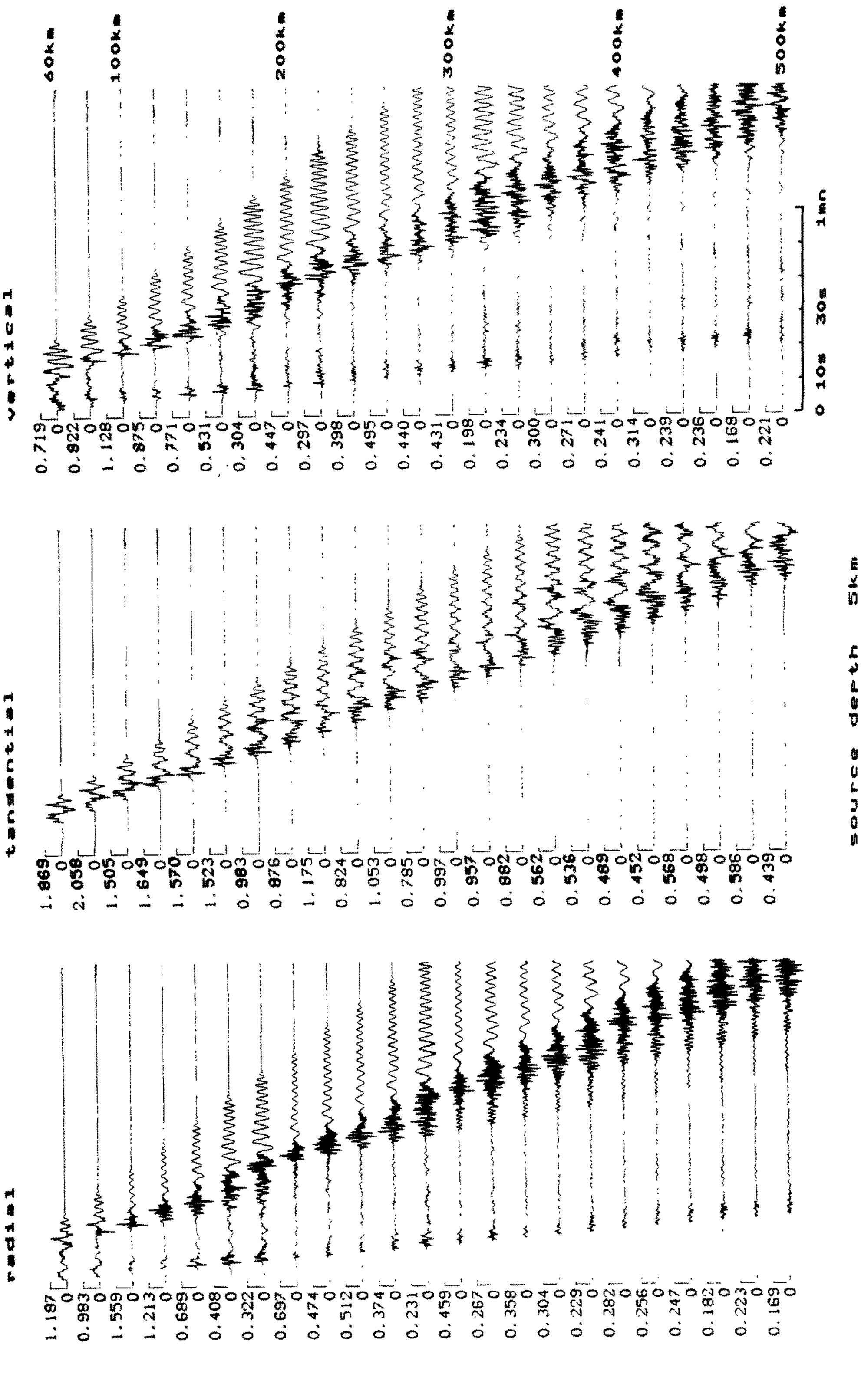

FIG. 1. Synthetic ground displacements produced by a vertical strike-slip point source for epicentral distances between 60 and 500 km at 20-km interval. The source depth is 5 km, and the source time function is defined by $[1 + \tanh(t/t_0)]/2$ with t_0 equal to 0.2 sec. The displacements are given in tenths of millimeters for a seismic moment of 10^{23} dyne-cm. The signal duration is 100 sec. Each trace is normalized by the peak value of displacement. The reduction velocity is 8 km/sec.

consists in a superposition of S waves multiply reflected within the crust and incident on the Moho at an angle more grazing than the critical angle. The energy of these waves is, therefore, trapped inside the crust. Similarly, the *Pg* wave group consists in a superposition of P waves reflected many times within the crust. The energy of these waves, however, is not efficiently trapped but leaks continuously into the mantle in the form of shear waves.

In order to further investigate the characteristics of these two phases, we have computed synthetic seismograms generated by earthquakes and explosions in the epicentral distance range extending from 60 to 500 km. Such an example is presented in Figure 1. The seismic source considered is a strike-slip dislocation occurring on a vertical fault and is represented by a point double couple having a smooth ramp function time dependance. The focal depth is 5 km, and the crustal model used for the calculation (Table 1) is representative of the structure of the crust in Central France (Perrier and Ruegg, 1973). The method of calculation provides complete synthetic seismograms between 0 Hz (static field) and the cutoff frequency which is taken equal to 5 Hz. The three groups of traces correspond to the radial, tangential, and vertical ground displacements nonconvolved with any instrument response.

TABLE 1

CRUSTAL MODEL

Layer Thickness (km)	P-Wave Velocity (km/sec)	S-Wave Velocity (km/sec)	Density (gm/cm^3)
2	4.5	2.6	2.6
16	6.0	3.5	2.8
6	6.3	3.65	2.9
6	6.7	3.9	3.1
	8.2	4.7	3.3

The amplitude scale is in tenths of millimeters for a seismic moment of 10^{23} dyne-cm. The profile lies at an azimuth of 30° relative to the fault strike. The waveforms of the three components, however, are independant of this angle which only affects the amplitude of the traces. The *Pg*, *Lg*, and surface wave groups are the major phases of the computed seismograms. The *Pn* and *Sn* arrivals are small in comparison and are only visible on some of the traces. *Lg* waves and Love waves strongly interfer on the tangential component. The ratio of maximum horizontal to vertical motion for *Lg* waves computed for each trace has a mean of 2.5. This result agrees well with the values inferred from short-period data which lie between 2 and 3 (Street and Turcotte, 1977; Street, 1978; Nuttli, 1979; Gupta *et al.*, 1982). As the amplitude ratio of SV to SH waves depends on the source mechanism and on the station azimuth, the value obtained in this study is only strictly valid for the particular mechanism and azimuth chosen. Because of the configuration considered here ($\theta = 30°$), however, this value should be close to the average theoretical value for a strike-slip source. Most remarkable is the large standard deviation obtained (0.9) which shows the great sensitivity of the ratio to the epicentral distance. Indeed, this deviation is only slightly smaller than the one measured on data (1.03) (Gupta *et al.*, 1982). The same observation holds when we compare the smallest and largest values of the amplitude ratio that we get (1.4 and 4.8) to the ones found by Gupta *et al.* (1982) (1.6 and 5.3). This indicates that small variations in epicental distance

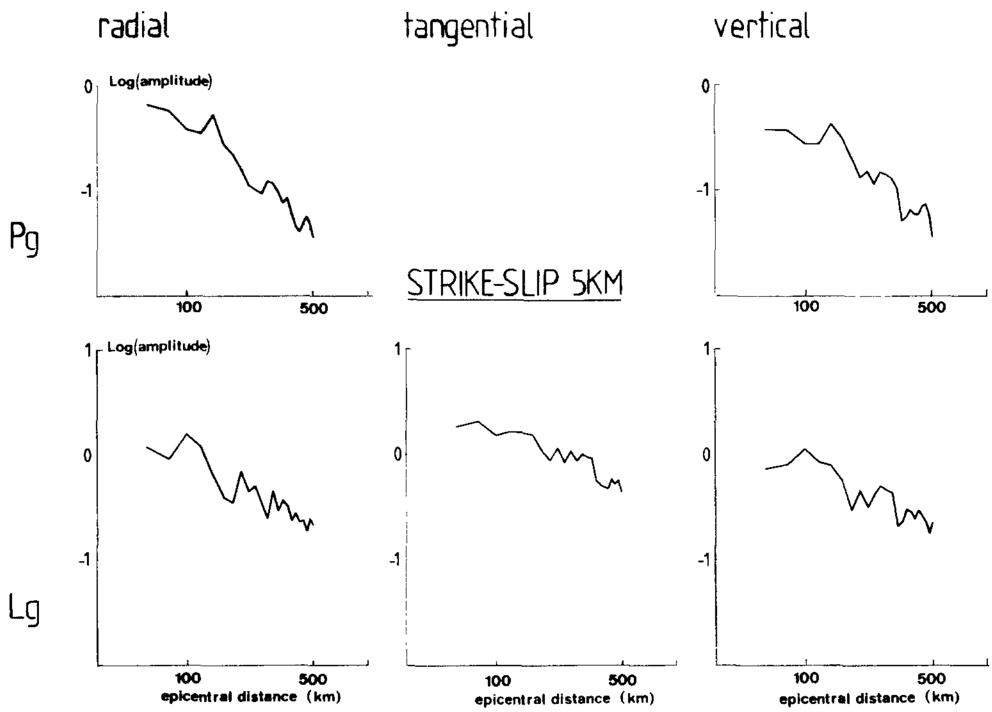

FIG. 2. Attenuation curves of *Pg* and *Lg* waves for each component of displacement for a strike slip source at a depth of 5 km.

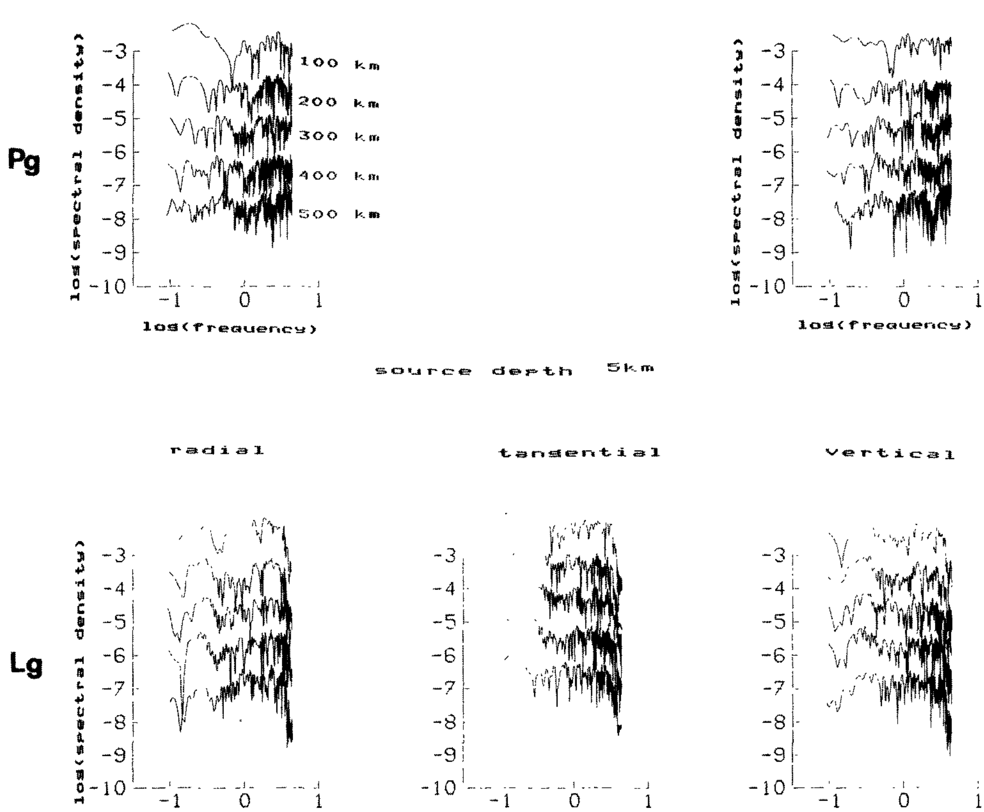

FIG. 3. Spectra of the crustal transfer function associated with *Pg* and *Lg* waves for a strike-slip source at a depth of 5 km. The time window is defined by group velocity between 6.5 and 4.0 km/sec for *Pg* and 3.8 and 2.5 km/sec for *Lg* waves. Five epicentral distances are considered from 100 to 500 km, and the corresponding spectra have been plotted with an arbitrary shift.

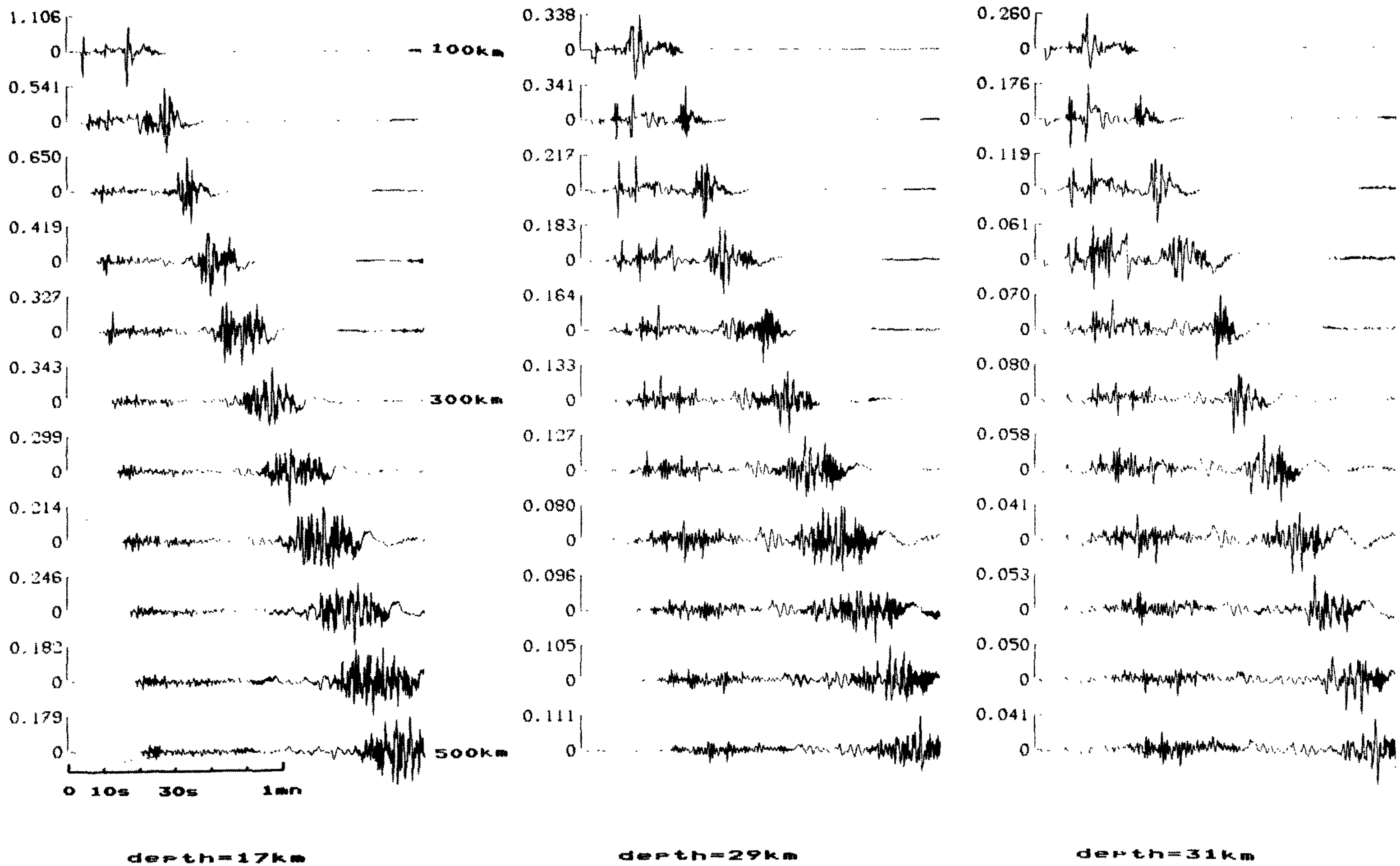

FIG. 4. Effect of the source depth on the seismic radiation from a vertical strike-slip earthquake. The vertical displacements are displayed for epicentral distances between 100 and 500 km at 40-km interval. The scales are the same as in Figure 1.

may affect the horizontal to vertical amplitude ratio as much as the changes of geology between sites which are present in the data.

The decay of maximum amplitude of the *Pg* and *Lg* wave groups with epicentral distance is displayed in Figure 2. As the calculations were done without any anelastic attenuation, these curves give the geometrical spreading characteristics of the two phases. They show that *Pg* waves attenuate with distance much more strongly than *Lg*. Another important feature is that, beyond 100 km, the amplitude decay of these phases is roughly the same on the three components. The slight higher attenuation rate of the horizontal component observed by Gupta *et al.* (1982) on short-period data is not apparent here.

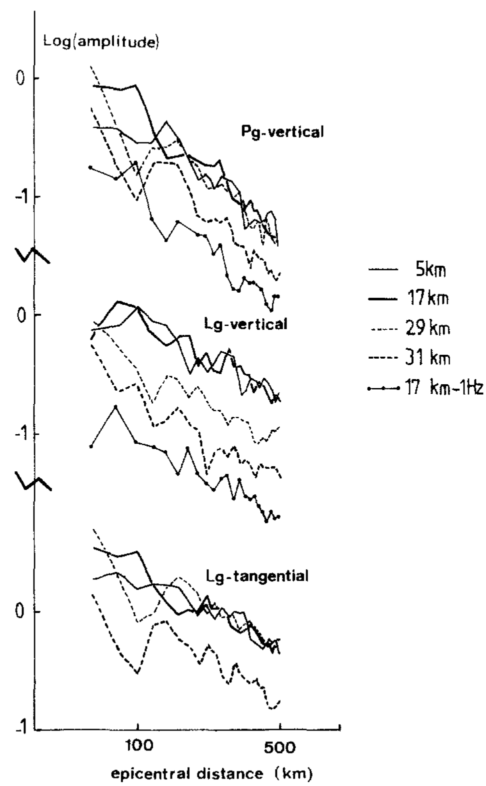

FIG. 5. Attenuation curves for a vertical strike-slip source at different depths. In the last case, the instrumental response is included.

Pg and *Lg* velocity spectra are shown in Figure 3, after deconvolution with the source time function. They represent the spectrum of the crustal transfer function for the two phases. The spectral shapes are independent of epicentral distance and are very similar on all the components. *Pg* wave spectra are flat over the frequency band considered which extends from 10 sec to 5 Hz while the *Lg* spectral amplitude, which is also roughly constant between 10 sec and 2 Hz, falls off very rapidly beyond 2 to 3 Hz. At 5 Hz, the *Lg* wave amplitude is about 10 to 50 times smaller than at 2 Hz. The higher low-frequency amplitude on the tangential component is due for a large part to Love wave contamination.

Effect of Source Depth

In order to understand how the depth of the source affects the excitation of *Pg* and *Lg* waves, we have repeated the previous calculation for different source depths:

17, 29, and 31 km. The synthetic seismograms corresponding to the vertical displacement are shown in Figure 4. As expected, the surface wave amplitude decreases strongly as the source depth increases. The amplitude of the *Pg* and *Lg* wave groups produced by a 17 km deep source are, on the average, about the same

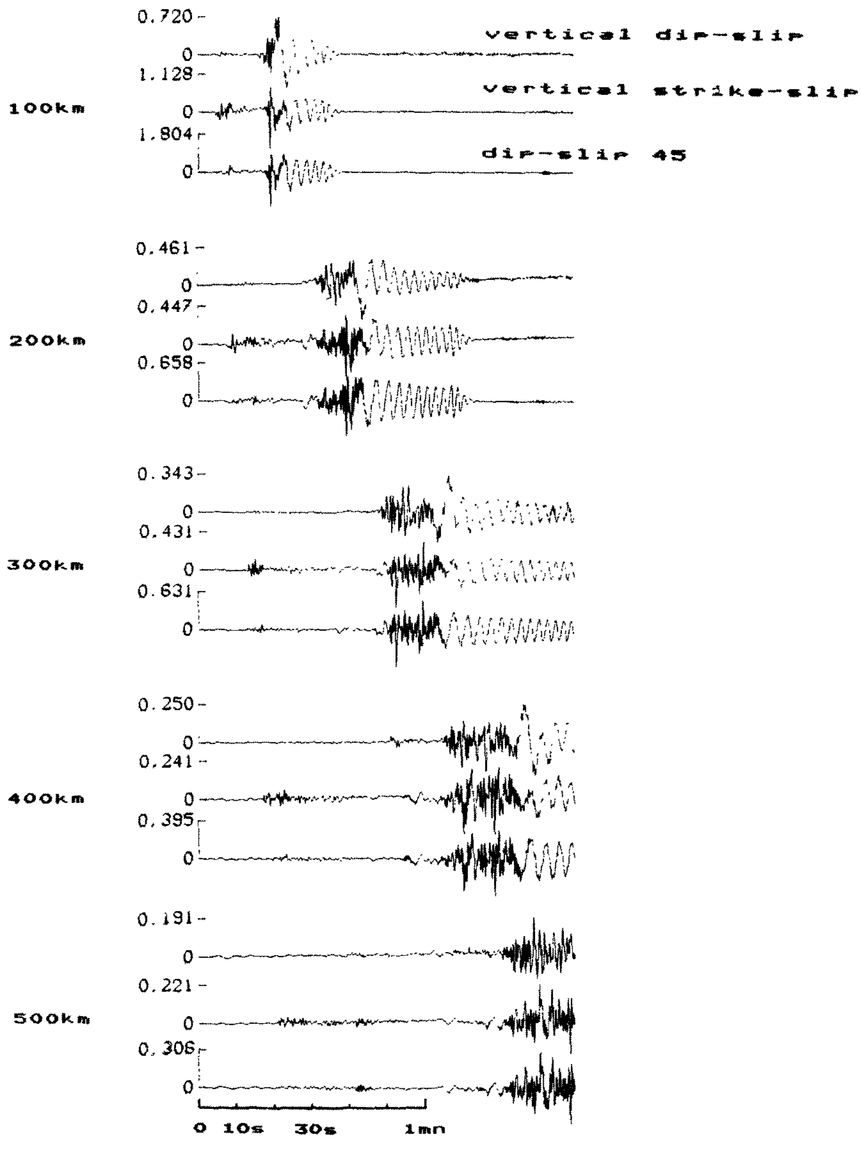

FIG. 6. Synthetic displacements produced by the three elementary types of seismic sources at five epicentral distances between 100 and 500 km. The scales are the same as in Figure 1. Note the similarity of the *Lg* waveforms radiated by a vertical strike slip and by a 45° dip slip.

as those obtained for a focal depth of 5 km. In contrast, when the source is located at the bottom of the crust (29 km), the *Lg* wave excitation is reduced by about 50 percent. The *Pg* wave amplitude, however, stays almost unchanged which results in a larger *Pg*-to-*Lg* amplitude ratio. The *Pg* wave excitation is insensitive to the location of the source within the crust while the *Lg* amplitude, at least for its *SV* component, is higher for a source in the upper or middle crust than in the lower crust. A similar dependency of *Lg* amplitude with source depth was found by Bache *et al.* (1981). When the source is located below the Moho (31 km), the amplitudes of *Pg* and *Lg* decrease drastically which confirms and illustrates the role of wave guide played by the crust for the propagation of these waves.

The curves of decrease of maximum amplitude with epicentral distance obtained for the four depths considered are presented in Figure 5. They show that beyond 100 km, the attenuation is independent of source depth. For *Lg* waves, the geometrical spreading inferred is of the form $r^{-0.83}$, where r denotes the epicentral distance. This value of the attenuation coefficient agrees remarkably well with the one assumed by Nuttli (1973) ($r^{-5/6}$ for the distance range considered here) and used in many subsequent studies. Nuttli's chosen coefficient corresponds to the theoretical

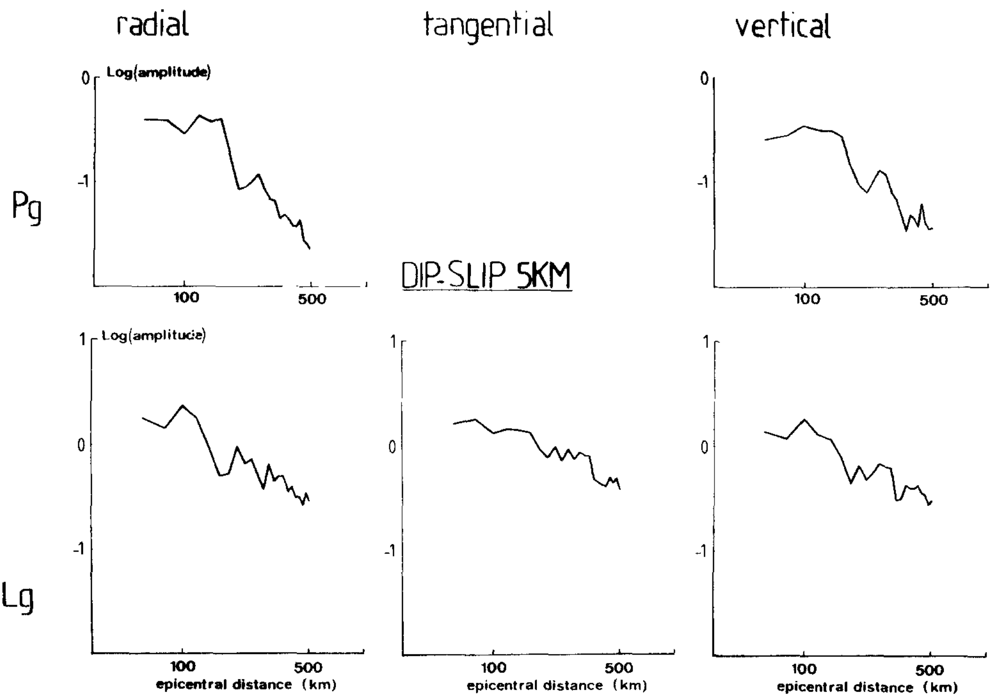

FIG. 7. Attenuation curves of *Pg* and *Lg* waves for each component of ground displacement for a thrust with a dip of 45° at a depth of 5 km.

attenuation of a dispersed Airy phase. The amplitude decay for the *Pg* waves is much faster than for *Lg* waves. The geometrical attenuation inferred is of the form $r^{-1.5}$. This value is similar to those obtained by Langston (1982) for a strike-slip source. These differences between *Pg* and *Lg* reflect their different modes of propagation.

In practice, the regional phases are observed on short-period vertical seismometers. To simulate these conditions, we have convolved the computed ground displacements with the response of an instrument having a 1-sec natural period. The corresponding curves of decay of peak amplitude are plotted on Figure 5 for a 17 km deep source: the decay is then the same as the one obtained for the ground motion.

EFFECT ON SOURCE MECHANISM

We present in Figure 6, the seismograms obtained for three different focal mechanisms: a vertical strike-slip dislocation, a thrust fault within a 45° dip, and a vertical dip-slip source. The solution for any other fault and slip orientation can be expressed as a superposition of the signals obtained for these three elementary sources. The focal depth considered is 5 km, and the profile of receivers lies at an azimuth of 30° relative to the fault strike. For the two dip-slip dislocation sources, the *Pg*-to-*Lg* amplitude ratio depends on the particular azimuth considered. A remarkable feature of the results is that the strike-slip source and the 45° thrust dislocation produce exactly superposable *Lg* waveforms.

In order to check the possible effect of source mechanism on the amplitude decay of *Lg* and *Pg* waves, we present in Figure 7 the curves of decrease of maximum

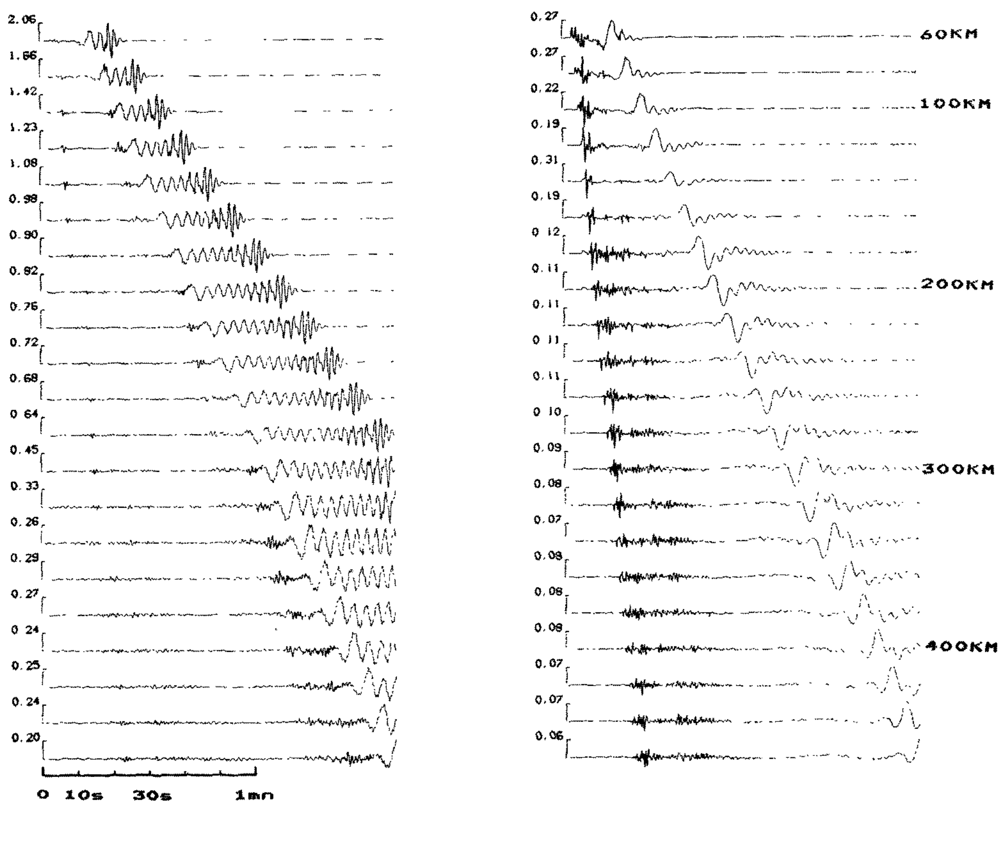

FIG. 8. Synthetic vertical displacements produced by an explosion at two different depths. The displacements are given in tenths of millimeters for a final pressure of 5 kbar at the source. The reduction velocity is 8 km/sec.

amplitude with epicentral distance for the thrust dislocation. A comparison with the strike-slip case (Figure 2) shows that, as expected, the *Lg* geometrical attenuations are, like the waveforms, exactly the same for the two sources. The *Pg* wave amplitude decay beyond 100 km is of the form $r^{-1.5}$, that is the same as the one inferred for the strike-slip source. The dependancy of *Pg* wave attenuation on source mechanism found by Langston (1982) on synthetized *Pg* is not present here. On the contrary, our results suggest that the geometrical attenuation of *Lg* and *Pg* is independent of source mechanism. A possible explanation for this discrepancy is that *Pg* wave are made up of interferences of numerous arrivals and may be difficult to describe fully with ray method. An incomplete representation of the wave field combined with different radiation patterns at the source could explain the dependency obtained by Langston.

EXCITATION OF *PG* AND *LG* WAVES BY AN EXPLOSIVE SOURCE

We now consider the case of an explosion. We model the seismic source as a pressure applied on the walls of a spherical cavity. We choose for the calculation a

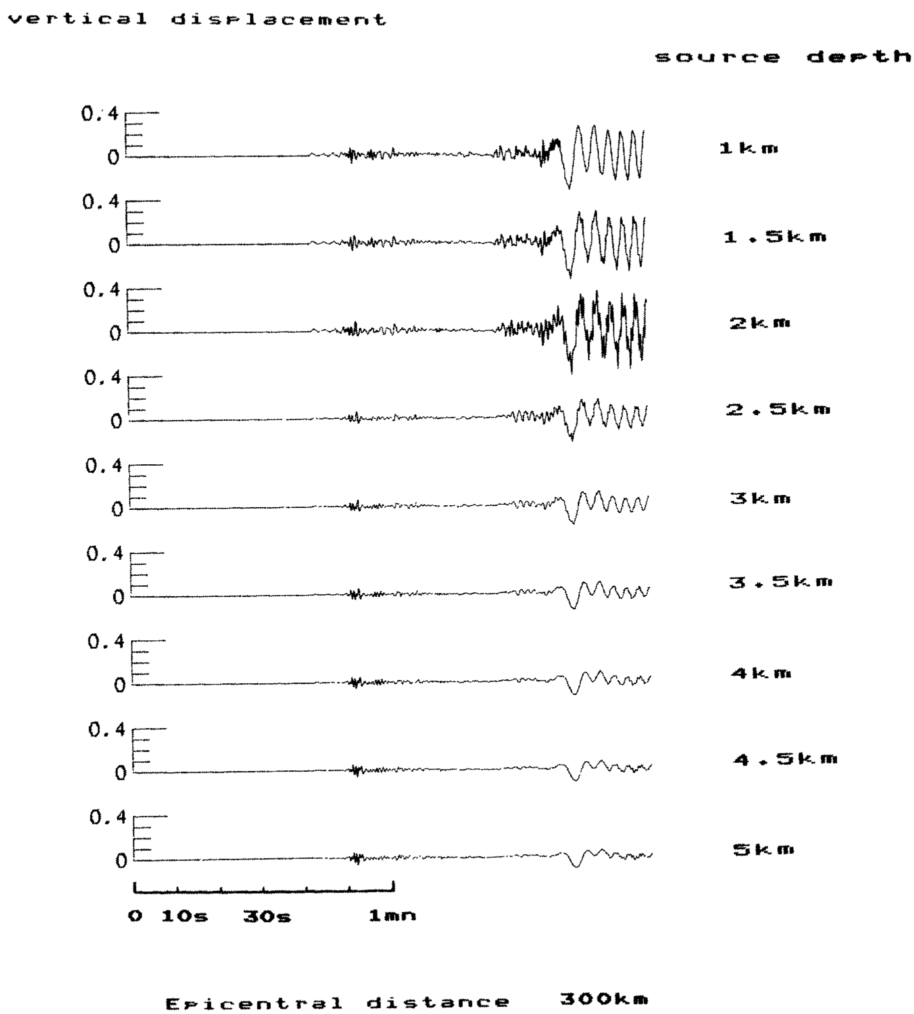

FIG. 9. Effect of explosion depth on vertical displacement produced at 300 km of epicentral distance. There is an interface at a depth of 2 km in the source model considered.

cavity radius of 100 m. The source time dependence is a smooth ramp function, and the final pressure is 5 kbar. The vertical ground displacements obtained are presented in Figure 8. Two different source depths are considered: 5 and 1.5 km. The former value allows a direct comparison with the seismograms obtained for the two types of sources previously considered. The most striking feature of the displacement traces produced by the deeper source is the almost total absence of the *Lg* phase. The same source located 1.5 km below the surface excites *Lg* waves, but their amplitude is small in comparison with *Pg* and Rayleigh waves. The short-period disturbance at the tail of the Rayleigh wave group is the Airy phase.

In order to better understand the effect of explosion depth on the generation of *Lg* waves, we have computed the surface displacement produced by a series of sources spanning the depth interval from 1 to 5 km. The results are presented in Figure 9. The *Pg* wave excitation is insensitive to the source depth within the interval considered. On the contrary, the *Lg* phase which is almost nonexistent for the 5 km deep source develops and increases in strength as the source depth decreases to 2 km. This depth corresponds to the interface between the sedimentary layer (V_p = 4.5 km/sec) and the basement crust (6 km/sec). Above 2 km, the amplitude of the *Lg* wave group stays about constant and roughly equal to the *Pg* wave amplitude.

These results suggest that the efficiency of *Lg* wave radiation by explosions depends on the closeness of the explosive source to the surface or to an interface. Irregularities in the interface shape will likely result in a stronger *P* to *S* conversion and further enhance the strength of the *Lg* waves radiated.

Conclusions

In order to better understand the generation and the propagation of regional seismic phases, we have computed complete seismograms in the distance range from 60 to 500 km, and we have studied the characteristics of the synthetized *Pg* and *Lg* waves. We have shown that the synthetics exhibit characteristics similar to the ones observed on data. We found that the geometrical spreading is of the form: $r^{-1.5}$ for *Pg* and $r^{-0.83}$ for *Lg* waves. We have computed the spectra of the crustal transfer function for these waves and shown that the spectra are flat for *Pg* waves between 10 sec and 5 Hz and display a strong high-frequency falloff beyond 2 to 3 Hz for *Lg* waves.

For a source within the crust, the *Pg* wave excitation is insensitive to the focal depth, while the strength of *Lg* waves is about 50 per cent weaker for a source in the lower crust than in the upper or middle crust. The amplitudes of both regional phases strongly decrease when the source is located below the Moho. These results support and illustrate the interpretation of *Lg* (or *Pg*) waves as *S* (or *P*) waves entirely (or partially) trapped in the crust. We have found that the source mechanism does not affect the geometrical attenuation of regional phases.

Considering the case of an explosive source, we have shown that, in presence of flat layers, the *Lg* waves are much weaker than *Pg* and Rayleigh waves. The excitation of *Lg* increases with the closeness of the source to an interface or to the free surface. At the same time, the *Pg* wave amplitude is insensitive to source depth.

Acknowledgments

This work was supported by the Advanced Research Projects Agency and was monitored by the Air Force Office of Scientific Research under Grant 80-0082.

References

Bache, T. C., H. J. Swanger, B. Shkoller, and S. M. Day (1981). Simulation of short period Lg, expansion of three dimensional source simulation capabilities and simulation of near-field ground motion from the 1971 San Fernando, California earthquake, Final Report, Systems, Science and Software, La Jolla, California.

Bollinger, G. A. (1979). Attenuation of the *Lg* phase and the determination of m_b in the southeastern United States, *Bull. Seims. Soc. Am.* **69,** 45–63.

Bouchon, M. (1981). A simple method to calculate Green's functions for elastic layered media, *Bull. Seism. Soc. Am.* **71,** 959–971.

Bouchon, M. (1982). The complete synthesis of seismic crustal phases at regional distances. *J. Geophys. Res.* **87,** 1735–1741.

Bouchon, M. and K. Aki (1977). Discrete wavenumber representation of seismic source wave fields, *Bull. Seism. Soc. Am.* **67**, 259–277.

Cara, M. and J. B. Minster (1981). Multi-mode analysis of Rayleigh-type *Lg*. Part 1. Theory and applicability of the method, *Bull. Seism. Soc. Am.* **71**, 973–984.

Gupta, I. N., B. W. Barker, J. A. Burnetti, and Z. A. Der (1980). A study of regional phases from earthquakes and explosions in western Russia, *Bull. Seism. Soc. Am.* **70**, 851–872.

Gupta, I. N., D. H. von Seggern, and R. A. Wagner (1982). A study of variation in the horizontal to vertical *Lg* amplitude ratio in the eastern United States, *Bull. Seism. Soc. Am.* **72**, 2081–2088.

Herrmann, R. B. and M. J. Goertz (1981). A numerical study of peak ground motion scaling, *Bull. Seism. Soc. Am.* **71**, 1963–1979.

Knopoff, L., F. Schwab, and E. Kausel (1973) Intepretation of *Lg*, *Geophys. J. R. Astron. Soc.* **33**, 983–993.

Kovach, R. L. and D. L. Anderson (1964). Higher mode surface waves and their bearing on the structure of the earth's mantle, *Bull. Seism. Soc. Am.* **54**, 161–182.

Langston, C. A. (1982). Aspects of Pn and Pg propagation at regional distances, *Bull. Seism. Soc. Am.* **72**, 457–471.

Müller, G. and S. Mueller (1979). Travel-time and amplitude interpretation of crustal phases on the refraction profile DELTA-W, Utah, *Bull. Seism. Soc. Am.* **69**, 1121–1132.

Nicolas, M., B. Massinon, P. Mechler, and M. Bouchon (1982). Attenuation of regional phases in western Europe, *Bull. Seism. Soc. Am.* **72**, 2089–2106.

Nuttli, O. W. (1973). Seismic wave attenuation and magnitude relations for eastern North America, *J. Geophys. Res.* **78**, 876–885.

Nuttli, O. W. (1979). The relation of sustained maximum ground acceleration and velocity to earthquake intensity and magnitude, State-of-the-art for assessing earthquake hazards in the United States, Report 16, Misc. paper S-73-1, U.S. Army Engineer Waterways Experiment Station, Vicksburg, Mississippi.

Nuttli, O. W. (1980). The excitation and attenuation of seismic crustal phases in Iran, *Bull. Seism. Soc. Am.* **70**, 469–485.

Nuttli, O. W. (1981). On the attenuation of *Lg* waves in western and central Asia and their use as a discriminant between earthquakes and explosions, *Bull. Seism. Soc. Am.* **71**, 249–261.

Oliver, J. and M. Ewing (1957). Higher modes of continental Rayleigh waves, *Bull. Seism. Soc. Am.* **47**, 187–204.

Oliver, J. and M. Ewing (1958). Normal modes of continental surface waves, *Bull. Seism. Soc. Am.* **48**, 33–49.

Olsen, K. H. and L. W. Braile (1983). Modeling short-period crustal phases ($\bar{P}$, *Lg*) for long-range refraction profiles, *Phys. of the Earth Planet Interiors* (in press).

Panza, G. F. and G. Calcagnile (1975). *Lg*, *Li* and *Rg* from Rayleigh modes, *Geophys. J. R. Astr. Soc.* **40**, 475–487.

Perrier, G. and J. C. Ruegg (1973). Structure profonde du Massif Central Français, *Ann. Geophys.* **29**, 435–502.

Pomeroy, P. W. and T. A. Nowak (1979). An investigation of seismic wave propagation in Western USSR, Semiannual Technical Report No. 2, Rondout Associates, Inc., Stone Ridge, New York.

Pomeroy, P. W. and T. C. Chen (1980). Regional seismic wave propagation, Final Report, Rondout Associates, Inc., Stone Ridge, New York.

Press, F. and M. Ewing (1952). Two slow surfaces waves across North America, *Bull. Seism. Soc. Am.* **42**, 219–228.

Street, R. L. (1978). A note on the horizontal to vertical *Lg* amplitude ratio in Eastern United States, *Earthquake Notes* **49**, 15–20.

Street, R. L. and F. T. Turcotte (1977). A study of northeastern North America spectral moments, magnitudes and intensities, *Bull. Seism. Soc. Am.* **67**, 599–614.

LABORATOIRE DE GÉOPHYSIQUE INTERNE
ERA CNRS 603
UNIVERSITÉ SCIENTIFIQUE ET MEDICALE DE GRENOBLE
BP 68, 38402 SAINT MARTIN D'HERES CEDEX, FRANCE (M.C., M.B.)

LABORATOIRES DE DETECTION ET DE GÉOPHYSIQUE
COMMISSARIAT A L'ENERGIE ATOMIQUE
BP 136, 92124 MONTOUGE CEDEX, FRANCE (B.M.)

Manuscript received 25 April 1983